Supplementary Material

Capillary force driven printing of asymmetric Na-ion micro supercapacitors

Jianmin Li, Yuanlong Shao, Chengyi Hou, Qinghong Zhang, Yaogang Li and Hongzhi Wang**

Figures

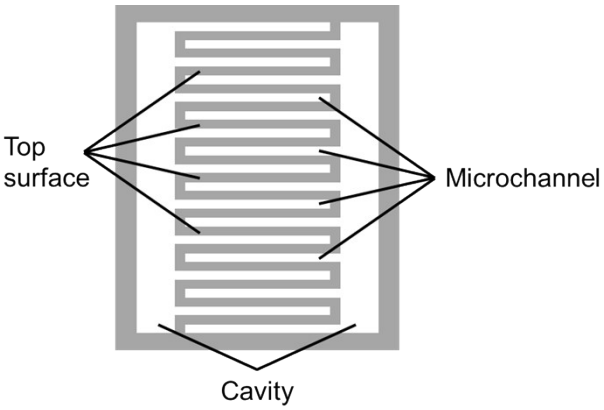

Fig. S1 The schematic diagram of the PDMS template. The white part and gray part represent the microgroove and PDMS, respectively.

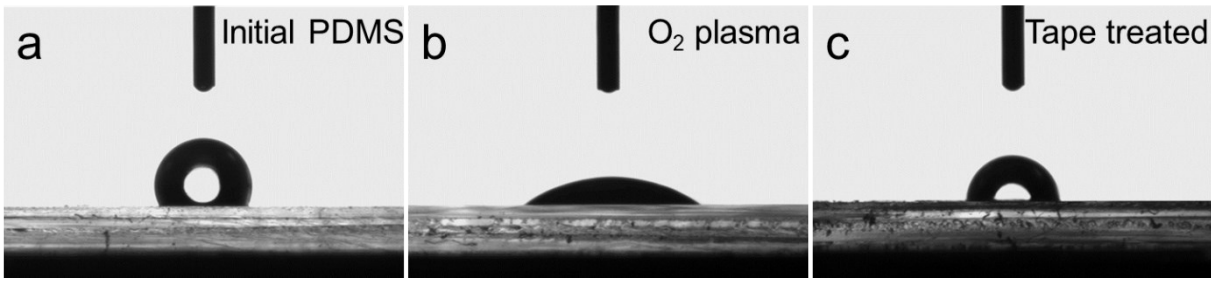

Fig. S2 Contact angle tests of PDMS film at different surface conditions: the initial state (a), after O_2 plasma treating (b) followed by the tape treatment (c).

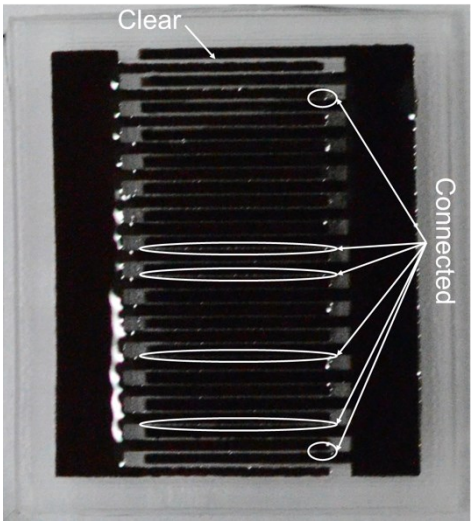

Fig. S3 Digital image of the just assembled device without tape treatment. Most of the gaps are interconnected with each other.

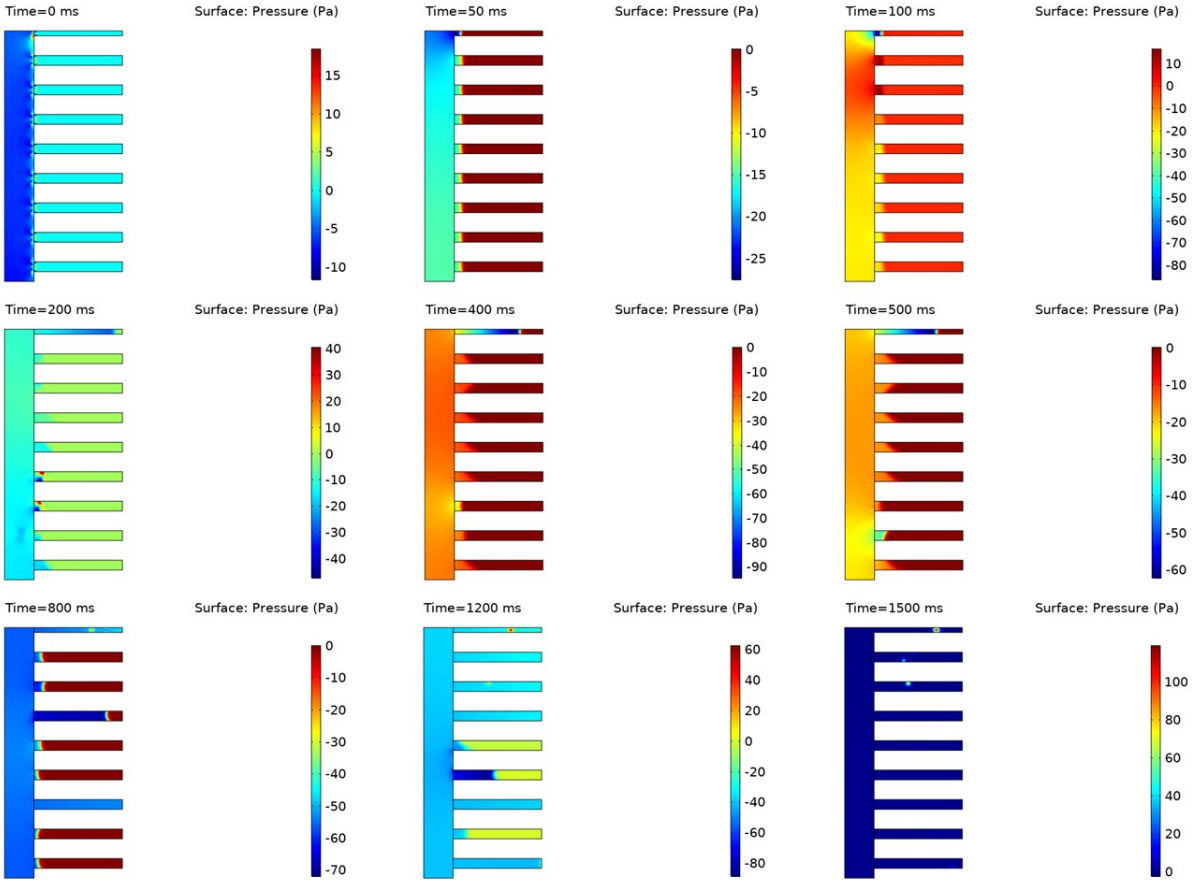

Fig. S4 The pressure field distribution of the electrode ink in the capillary during the fabrication process.

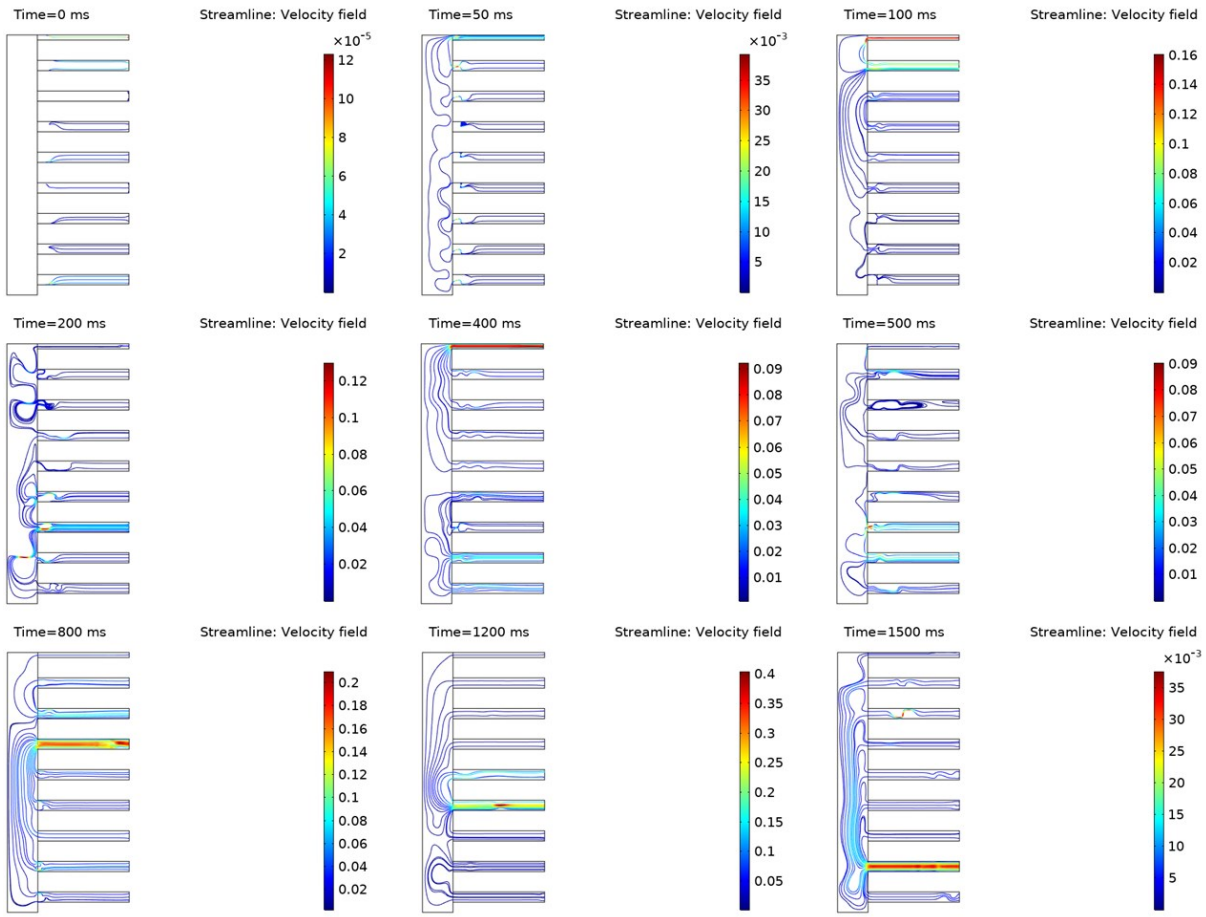

Fig. S5 The velocity field distribution of the electrode ink in the capillary during the fabrication process.

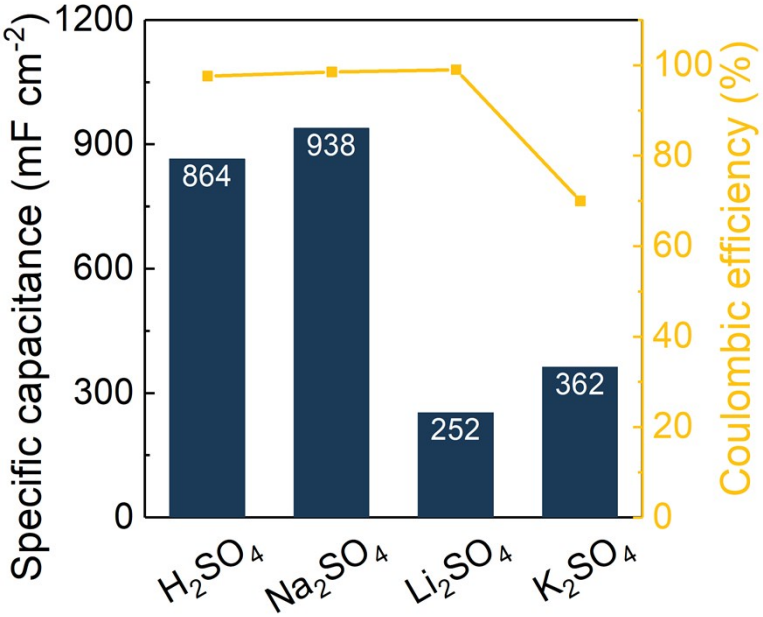

Fig. S6 Capacitance and coulombic efficiency of the SWCNTs/PEDOT:PSS/CuHCF film tested in different electrolytes.

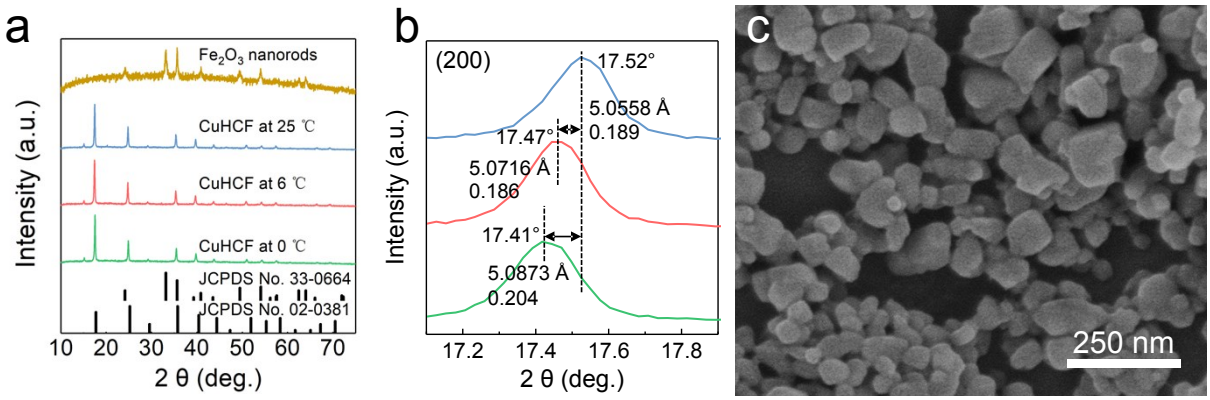

Fig. S7 XRD patterns of (a) Fe_2O_3 NRs and CuHCF NPs synthesized at different temperatures, and (b) partially magnified (200) peak of the CuHCF NPs. (c) SEM image of the CuHCF NPs synthesized at 0°C.

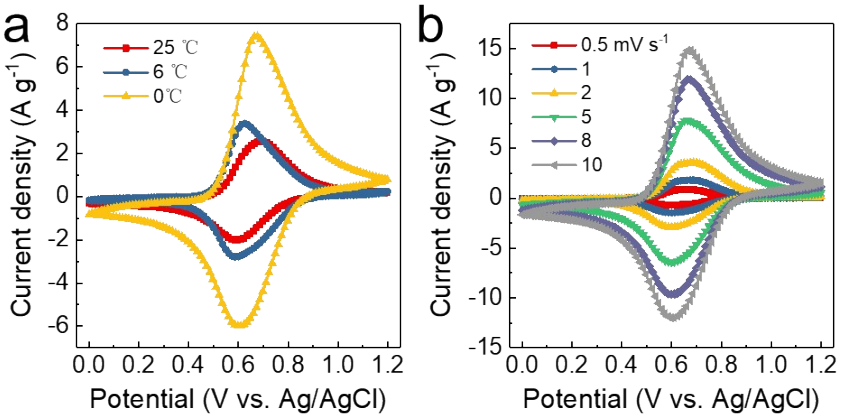

Fig. S8 Cyclic voltammetry curves of the CuHCF NPs: (a) synthesized at different temperature, scan rate: 10 mV s^{-1}; (b) synthesized at 0 ℃ under various scan rates.

To further enhance the electrochemical performance of the CuHCF NPs, we synthesized it at different temperatures (25℃, 6℃ and 0℃), whose X-ray diffraction (XRD) patterns were shown in Fig. S7a. It is obvious that all of these three samples are well-crystallized cubic phase CuHCF, with the typical diffraction peaks located around 17.5, 25.2, 35.7 and 40.4°, indexing as (200), (220), (400) and (420) reflections (JCPDS No. 02-0381). We then magnified the (200) peak to ulteriorly evaluate the influence of temperature (see Fig. S7b), from which a left shift of the peak position is obvious as the temperature decreasing. Moreover, the interplanar spacing of these three samples were obtained by *Bragg equation*:

$$2d\sin\vartheta=n\lambda \qquad \text{(S1)}$$

where d is the interplanar spacing, ϑ is the diffraction angle, n is the diffraction series (n=1), λ is the wavelength (λ=1.5406 Å). Its interplanar spacing increased to 5.0873 Å at 0℃ from 5.0558 Å at 25℃, which is beneficial for the hydrated Na^+ to insert. Fig. S7c exhibited the SEM image of the CuHCF NPs synthesized at 0℃, indicating the cubic morphology. As a result, the optimized electrochemical property was obtained for the CuHCF NPs synthesized at 0℃, as well as the outstanding rate capability (Fig. S8). Thus, the CuHCF NPs synthesized at 0℃ was selected as the activated materials of positive electrode.

The XRD pattern of Fe_2O_3 NRs is shown in Fig. S7a, from which the peaks located at 24.1, 33.2, 35.6 and 39.3° can be indexed as (012), (104), (110) and (006) reflections (JCPDS No. 33-0664) of hexagonal phase Fe_2O_3.

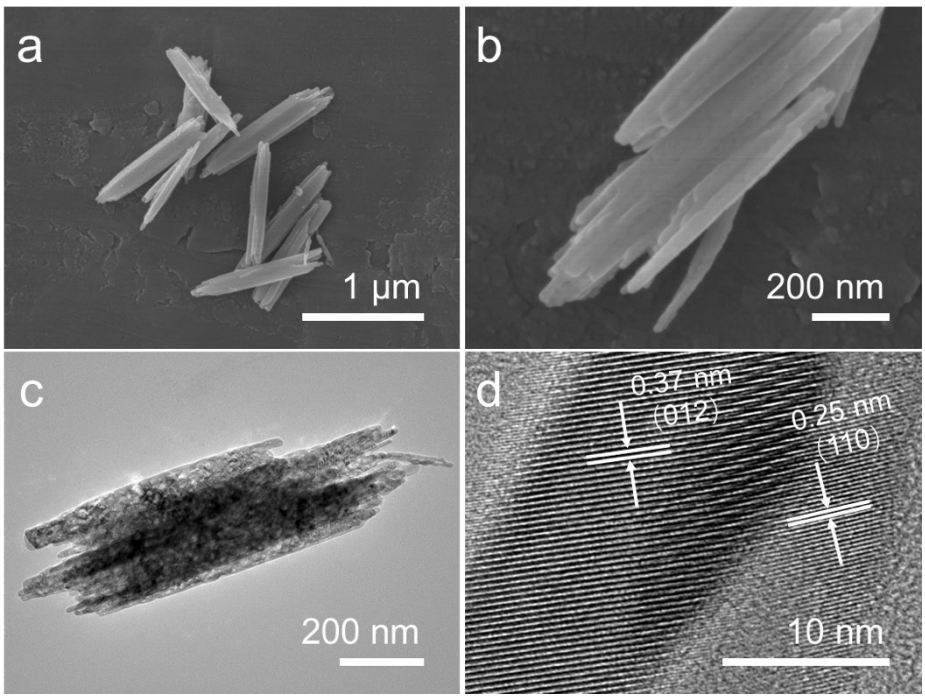

Fig. S9 (a, b) SEM images, (c) TEM image and (d) HRTEM image of the as prepared Fe_2O_3 NRs.

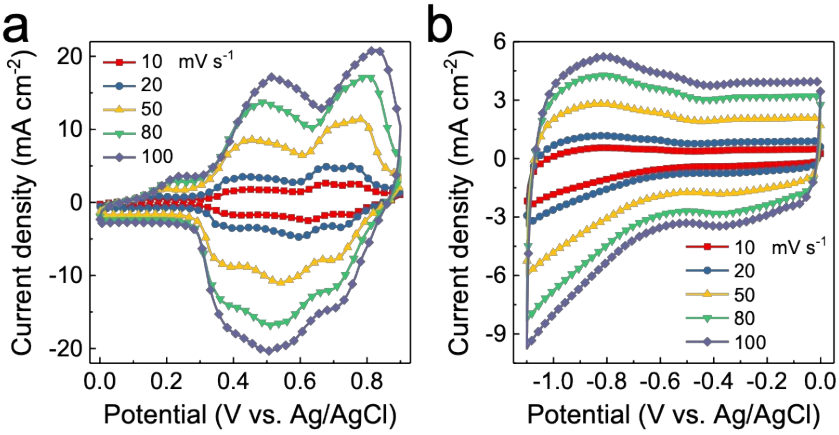

Fig. S10 The cyclic voltammetry curves of the 2-μm SWCNTs/PEDOT:PSS/CuHCF film (a) and SWCNTs/PEDOT:PSS/Fe_2O_3 film (b).

Fig. S10a shows the CV curves (scan rate: 10-100 mV s^{-1}) of the as prepared SWCNTs/PEDOT:PSS/CuHCF film. It is obvious that the film showed a significant pseudocapacitive behavior, with two pairs of redox peaks, which are maintained even at a high scan rate of 100 mV s^{-1}. Its specific capacitance was calculated to be 158 mF cm^{-2} at 10 mV s^{-1}, retaining 85.4% of its initial capacitance (135 mF cm^{-2}) under the scan rate of 100 mV s^{-1}.

Also, we have prepared a SWCNTs/PEDOT:PSS/Fe_2O_3 composite film, with a thickness of 2 μm, to verify its potential to be used as the negative electrode of an AMSCs. From the CV curves shown in Fig. S10b, a wide voltage window of -1.1 V (-1.1~0 V) was clearly observed, as well as the intercalation-induced pseudocapacitive nature. It is striking that the ternary film can deliver a high areal specific capacitance of 77 F cm^{-2} at scan rate of 10 mV s^{-1}. Notably, as a result of its high conductivity, the ternary film could still maintain 67 F cm^{-2} at 100 mV s^{-1}, indicating a great rate performance. The energy storage mechanism could be summarized by the following equation:

$$Fe_2O_3 + xNa^+ + xe^- \leftrightarrow Na_xFe_2O_3 \quad \text{(S2)}$$

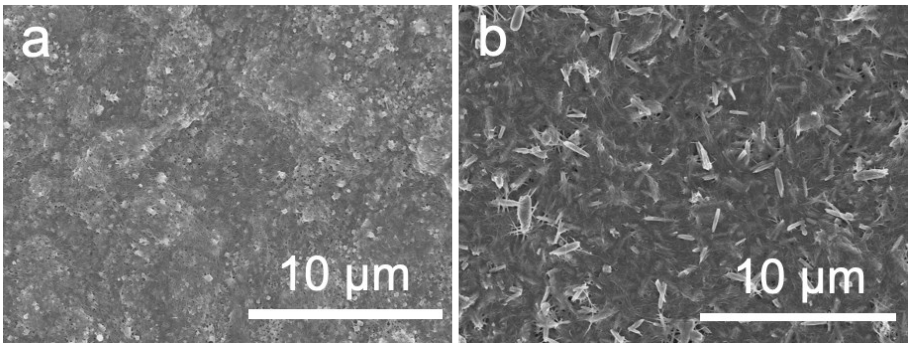

Fig. S11 SEM images of positive electrode (a) and negative electrode (b).

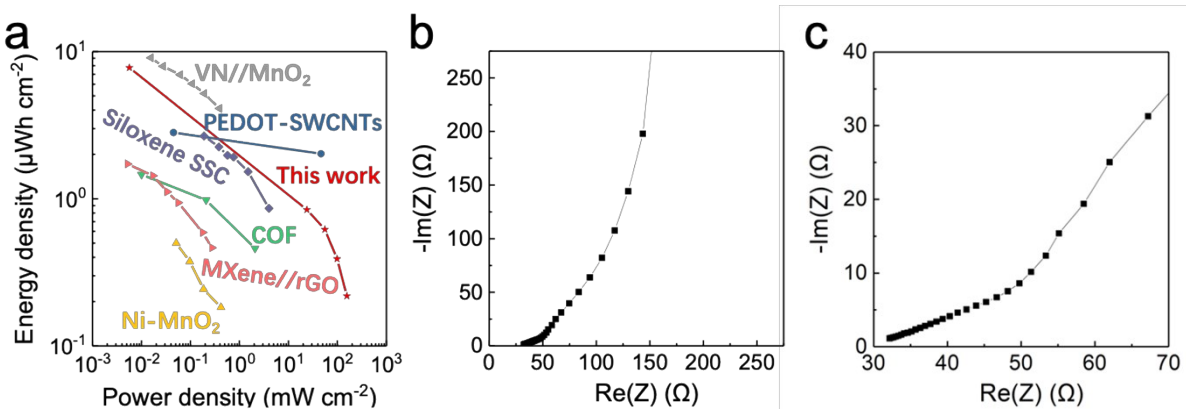

Fig. S12 Ragone plot (a), Nyquist plot (b), and enlarged Nyquist plot (c) of the as prepared AMSCs. SSC: symmetric supercapacitor, COF: Covalent Organic Frameworks, rGO: reduced graphene oxide.

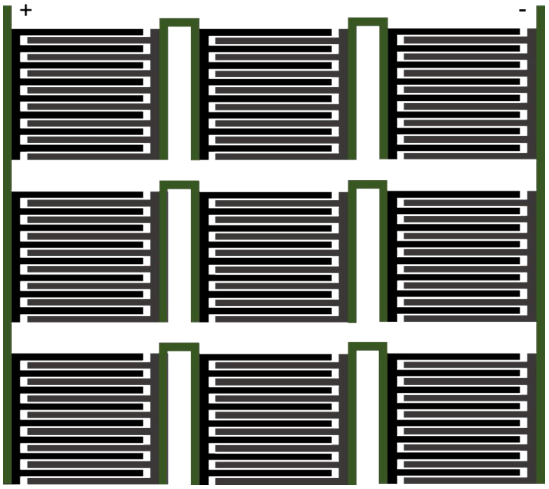

Fig. S13 The schematic diagram of the 9-device connected array.

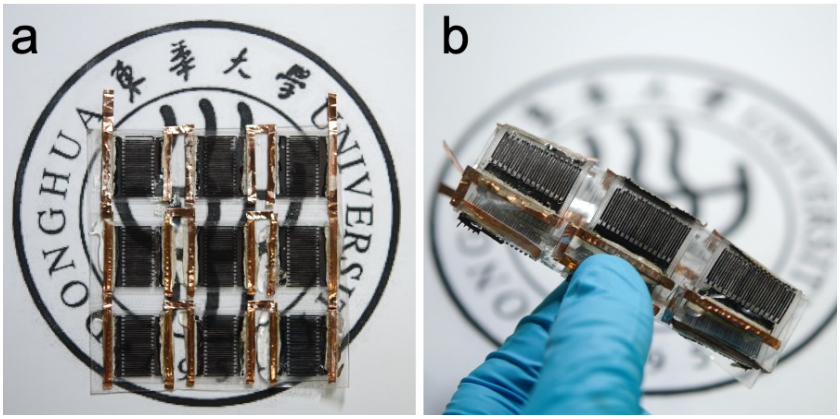

Fig. S14 Digital images of the 9-device connected array.